Unique, Gender-Dependent Serum microRNA Profile inPLS3 Gene-Related Osteoporosis

Mäkitie, Riikka E.

2020-10

Mäkitie , R E , Hackl , M , Weigl , M , Frischer , A , Kämpe , A , Costantini , A , Grillari , J & Mäkitie , O 2020 , ' Unique, Gender-Dependent Serum microRNA Profile inPLS3 Gene-Related Osteoporosis ' , Journal of Bone and Mineral Research , vol. 35 , no. 10 , pp. 1962-1973 . https://doi.org/10.1002/jbmr.4097

http://hdl.handle.net/10138/320787
https://doi.org/10.1002/jbmr.4097

ORIGINAL ARTICLE

JBMR®

Unique, Gender-Dependent Serum microRNA Profile in *PLS3* Gene-Related Osteoporosis

Riikka E Mäkitie,[1,2,3] Matthias Hackl,[4,5] Moritz Weigl,[4] Amelie Frischer,[5,6] Anders Kämpe,[7,8] Alice Costantini,[7,8] Johannes Grillari,[5,6,9] and Outi Mäkitie[1,2,7,8,10]

[1]Folkhälsan Institute of Genetics, University of Helsinki, Helsinki, Finland
[2]Research Program for Clinical and Molecular Metabolism, Faculty of Medicine, University of Helsinki, Helsinki, Finland
[3]Molecular Endocrinology Laboratory, Department of Metabolism, Digestion and Reproduction, Hammersmith Campus, Imperial College, London, London, United Kingdom
[4]TAmiRNA GmbH, Vienna, Austria
[5]Austrian Cluster of Tissue Regeneration, Vienna, Austria
[6]Ludwig Boltzmann Institute for Experimental and Clinical Traumatology, Vienna, Austria
[7]Department of Molecular Medicine and Surgery, Karolinska Institutet, Stockholm, Sweden
[8]Clinical Genetics, Karolinska University Hospital, Stockholm, Sweden
[9]Christian Doppler Laboratory on Biotechnology of Skin Aging, Institute of Molecular Biotechnology, Department of Biotechnology, BOKU–University of Natural Resources and Life Sciences Vienna, Vienna, Austria
[10]Children's Hospital and Pediatric Research Center, University of Helsinki and Helsinki University Hospital, Helsinki, Finland

ABSTRACT

Plastin 3 (PLS3), encoded by *PLS3*, is a newly recognized regulator of bone metabolism, and mutations in the encoding gene result in severe childhood-onset osteoporosis. Because it is an X chromosomal gene, *PLS3* mutation-positive males are typically more severely affected whereas females portray normal to increased skeletal fragility. Despite the severe skeletal pathology, conventional metabolic bone markers tend to be normal and are thus insufficient for diagnosing or monitoring patients. Our study aimed to explore serum microRNA (miRNA) concentrations in subjects with defective PLS3 function to identify novel markers that could differentiate subjects according to mutation status and give insight into the molecular mechanisms by which PLS3 regulates skeletal health. We analyzed fasting serum samples for a custom-designed panel comprising 192 miRNAs in 15 mutation-positive (five males, age range 8–76 years, median 41 years) and 14 mutation-negative (six males, age range 8–69 years, median 40 years) subjects from four Finnish families with different *PLS3* mutations. We identified a unique miRNA expression profile in the mutation-positive subjects with seven significantly upregulated or downregulated miRNAs (miR-93-3p, miR-532-3p, miR-133a-3p, miR-301b-3p, miR-181c-5p, miR-203a-3p, and miR-590-3p; *p* values, range .004–.044). Surprisingly, gender subgroup analysis revealed the difference to be even more distinct in female mutation-positive subjects (congruent *p* values, range .007–.086) than in males (*p* values, range .127–.843) in comparison to corresponding mutation-negative subjects. Although the seven identified miRNAs have all been linked to bone metabolism and two of them (miR-181c-5p and miR-203a-3p) have bioinformatically predicted targets in the *PLS3* 3′ untranslated region (3′-UTR), none have previously been reported to associate with PLS3. Our results indicate that *PLS3* mutations are reflected in altered serum miRNA levels and suggest there is crosstalk between PLS3 and these miRNAs in bone metabolism. These provide new understanding of the pathomechanisms by which mutations in *PLS3* lead to skeletal disease and may provide novel avenues for exploring miRNAs as biomarkers in PLS3 osteoporosis or as target molecules in future therapeutic applications. © 2020 The Authors. *Journal of Bone and Mineral Research* published by American Society for Bone and Mineral Research.

KEY WORDS: BIOCHEMICAL MARKERS OF BONE TURNOVER; CELL/TISSUE SIGNALING – PARACRINE PATHWAYS; GENETIC RESEARCH; OSTEOGENESIS IMPERFECTA; OSTEOPOROSIS

Received in original form January 23, 2020; revised form May 14, 2020; accepted May 20, 2020; Accepted manuscript online May 26, 2020.

Address correspondence to: Riikka E Mäkitie, MD, PhD, Folkhälsan Institute of Genetics, P.O. Box 63, FIN-00014 University of Helsinki, Helsinki, Finland. E-mail: riikka.makitie@helsinki.fi

Additional Supporting Information may be found in the online version of this article.

Journal of Bone and Mineral Research, Vol. 35, No. 10, October 2020, pp 1962–1973.
DOI: 10.1002/jbmr.4097

Introduction

In recent years, large-scale sequencing efforts and advanced next-generation sequencing methods have enabled recognition of several genetic factors and loci that associate with bone quality and fracture risk and contribute to various skeletal pathologies.[1–5] Nevertheless, understanding the complexities of the human genome has proven difficult. Today, non-protein–coding genomic components are considered to have an important, disease-modulating role.[6–8] As such, microRNAs (miRNAs)—short, non-coding RNA fragments—play an integral role in various biological processes by regulating gene expression and protein translation by posttranscriptional silencing or repression.[9] In bone, miRNAs affect osteogenic cell maturation and function directly, and thus partake in fetal skeletal development and maintenance of postnatal bone health.[10–12] miRNAs are also clinically valued because differences in serum miRNA levels correlate with disease status and mirror disease progression, differentiate between patient cohorts, and will, possibly, offer new means of target treatments in the near future.[8,13–15] We have previously reported altered miRNA concentrations in a monogenic skeletal disorder, WNT1 osteoporosis, and shown that a unique miRNA pattern differentiates patients according to their mutation status.[8] However, the significance and value of miRNAs in other rare, monogenic bone diseases is still incompletely explored.

Plastin 3, encoded by X chromosomally inherited *PLS3*, is a newly recognized regulator of bone metabolism. In 2013, loss-of-function mutations in *PLS3* were identified as the cause for severe childhood-onset, X-linked primary osteoporosis.[16] Hemizygous males are commonly more severely affected and sustain multiple low-energy peripheral and vertebral compression fractures starting at an early age.[17–20] The phenotype in heterozygous females varies from normal to increased skeletal fragility.[17–20] Bone biopsies portray low turnover osteoporosis with scarce bone cells, decreased bone formation, and heterogenous and defective matrix mineralization.[17,19] Although, to date, many other patients and families worldwide have been identified with *PLS3* mutations and patients' clinical skeletal characteristics are well documented,[21] the main molecular mechanisms and pathways through which PLS3 regulates and diverges with in bone metabolism remain elusive.

To date, we have identified altogether four unrelated Finnish families with PLS3 osteoporosis caused by different *PLS3* mutations.[18–20] We and others have previously reported that despite the manifest bone pathology, conventional metabolic bone markers are normal in *PLS3* mutation-positive patients and hence offer no aid in clinical diagnosis or follow-up.[19] We hypothesized that abnormal PLS3 function due to *PLS3* mutations is reflected in serum miRNA expression levels and therefore set out to evaluate affected patients' serum miRNA expression profiles with the objective to distinguish probable new biomarkers and shed light on the molecular pathomechanisms in PLS3-related skeletal disorders.

Subjects and Methods

Subjects

We have previously identified four Finnish families with X-linked PLS3 osteoporosis due to different mutations in *PLS3* (Fig. 1).[18–20] The first family (Family A) has an intronic splice site mutation c.73–24T>A (p.Asp25Alafs*17) identified by exome

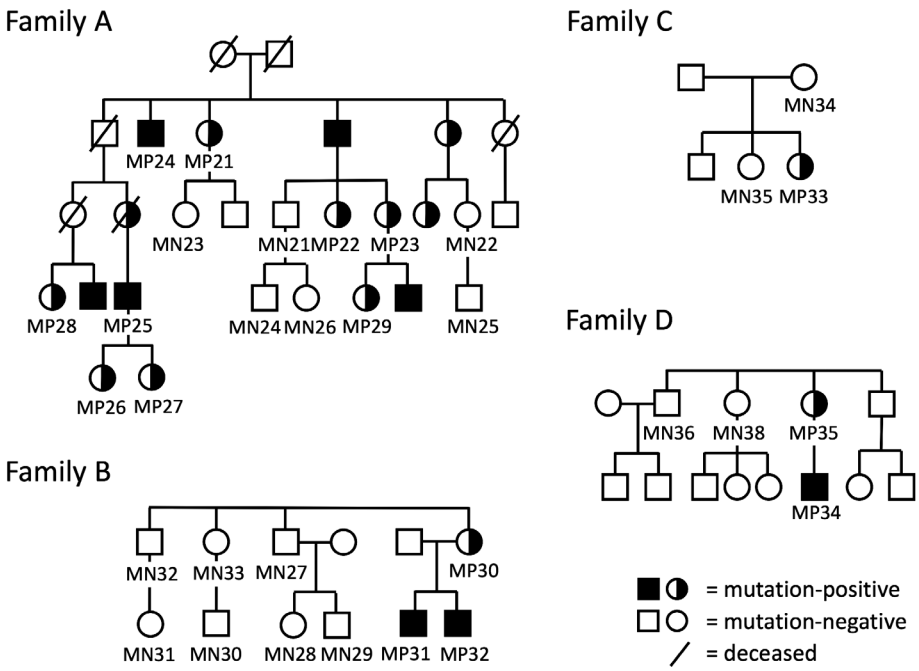

Fig 1 Pedigrees of the four included Finnish families with *PLS3* mutations. Family A: intronic splice-site mutation c.73–24T>A (p.Asp25Alafs*17); Family B: intragenic tandem duplication within *PLS3*; Family C: *de novo* heterozygous missense mutation c.1424A>G (p.Asn446Ser); and Family D: nonsense mutation c.766C>T (p.Arg256*). The pedigrees have been modified to ensure anonymity. Squares represent males, circles females. MN = mutation-negative; MP = mutation-positive.

sequencing as described.[19] The second family (Family B) includes three subjects with an intragenic tandem duplication within *PLS3* as identified by genomic hybridization array (array-CGH).[20] The third family (Family C) consists of a single subject with a *de novo* heterozygous missense mutation c.1424A>G (p.Asn446Ser) in exon 12 identified by Sanger sequencing of the whole *PLS3* gene as described.[18] Last, the fourth family (Family D) includes two subjects with a nonsense mutation c.766C>T (p.Arg256*) in exon 8, also identified by conventional Sanger sequencing of the whole *PLS3* gene.[18]

Since initial recognition of each family's mutation, we have offered genetic screening to all first-degree family members and hence, to date, we have identified altogether 21 *PLS3* mutation-positive individuals in these four families (Family A, $n = 15$; Family B, $n = 3$; Family C, $n = 1$; and Family D, $n = 2$). For the current study, we offered all mutation-positive individuals ($n = 20$; one deceased) the opportunity to take part in a study concerning new bone biomarkers in PLS3 osteoporosis. To form a comparable control group with a similar genetic background as well as age and gender distribution, we also offered participation to the mutation-negative individuals ($n = 31$) from these four families. In total 15 mutation-positive and 17 mutation-negative individuals consented. All subjects or their legal guardians gave a written informed consent upon participation in the study. The research protocol was approved by the Research Ethics Board of Helsinki University Hospital.

Each participant completed a questionnaire concerning other chronic illnesses, previous fractures, orthopedic surgeries, osteoporosis and other long-term medications, and calcium and vitamin D supplementation. All anamnestic data were reviewed for possible confounding factors regarding miRNA expression levels.

Genetic evaluations

We have previously screened all participating individuals for the families' pertinent *PLS3* mutations. Genetic validations were performed on DNA extracted from peripheral blood as described.[18–20]

Serum samples

We collected serum samples from all subjects during the summer months (June–August) in 2017 to avoid seasonal bias from variable sunlight exposure. We collected all samples after an overnight fast, in the morning between 8:00 a.m. and 9:00 a.m. First, we collected venous peripheral blood in normal serum tubes, let them stand and clot at room temperature for 30–60 min, and then centrifuged them at 2500*g* for 10 min. The supernatants were then transferred to 1.5-mL tubes in 250-μL aliquots and stored immediately at −80°C until analysis.

Blood biochemistry

We have previously measured basic biochemistry and conventional bone metabolic markers for each subject. These included serum ionized calcium, phosphate, alkaline phosphatase (ALP), and 25-hydroxyvitamin D (S-D-25) (assessed with immunochemiluminometry) at HUSLAB Laboratory (Helsinki, Finland). Parathyroid hormone (PTH) and bone resorption marker collagen type 1 cross-linked C-telopeptide (CTX-1) were both assessed from serum with an IDS-iSYS fully automated immunoassay system (Immunodiagnostic Systems, Ltd., Bolton, UK). For each parameter, results were compared with the laboratory's or manufacturer's reference values. All were measured from blood, serum, or plasma samples collected in parallel with the samples for the miRNA analyses.

miRNA analyses

Serum was thawed at room temperature and centrifuged at room temperature for 5 min at 12,000*g* to remove cellular debris. RNA extraction was performed using precisely 200 μL serum as described[8,15] using the miRNeasy Mini Kit (Qiagen, Hilden, Germany) with the following modification: synthetic, nonhuman oligonucleotides (Qiagen) were added to the Qiazol lysis buffer, glycogen was added to the precipitation at a final concentration of 0.5 mg/mL to enhance precipitation, and columns were washed three times with ethanol before elution in 30 μL nuclease-free water. Eluted total RNA was stored at −80°C until further analysis.

Four microliters (4 μL) of total RNA were mixed with cel-miR-39 (RT spike-in control; Qiagen) and used for reverse transcription (RT) using the miRCURY RT kit (Qiagen) in 10-μL reactions at 42°C for 60 min. The resulting cDNA was overall diluted 1:100 for qPCR analysis using the 2× miRCURY SYBR Green mix and nuclease-free water (Qiagen). qPCRs were performed in 10-μL reactions using custom designed 384-well plates with dried miRCURY LNA primers (Qiagen) targeting 192 different miRNAs and quality controls per sample. Forty-five qPCR cycles were performed according to the manufacturer's instructions for two-step protocols optimized for Roche LC480 II instruments (Roche Diagnostics, Mannheim, Germany). The resulting fluorescence data were used to derive cycle quantification (Cq) values using the second derivative method. Cq values for RNA, RT, and PCR spike-in controls were visually inspected to identify samples where analysis had failed. Hemolysis was judged based on the ratio between miR-23a-3p and miR-451a, according to Blondal and colleagues.[22] Samples with high quality were selected for further analysis, for which global mean normalization was performed based on the average Cq signal, as calculated based on the signals from all detected ($Cq < 40$) miRNAs per sample.

We screened all serum samples with a previously described analytical workflow for 192 distinct miRNA species and controls.[8,15] The primary outcomes of interest were the top 10% of most differentially expressed miRNAs and the number and type of significantly differentially expressed miRNAs specific to subjects with *PLS3* mutations. The specific miRNAs represent an unbiased selection of the most abundant and measurable miRNAs in human serum or plasma.[8,15] We added spike-in controls prior to RNA extraction, RT, and qPCR amplification to evaluate possible technical variance of the workflow and to detect potential outliers. To exclude the possibility that results would be biased by hemolysis, we calculated a hemolysis index from the ratio of miR-451a and miR-23a-3p, as described by Blondal and colleagues.[22] miRNA target prediction was performed using TargetScan (v7.2) (https://lens.elifesciences.org/05005/index.html) and miRWalk (v3.0)[23] using the default parameters. Gene set enrichment analysis (GSEA) was performed using miRWalk (v3.0) using the default parameters and intersection with TargetScan prediction. Experimental design, protocols, and raw and normalized RT-qPCR data have been submitted to NCBI Gene Expression Omnibus (accession number GSE142872; https://www.ncbi.nlm.nih.gov/geo/query/acc.cgi?acc=GSE142872) to enable public access to our dataset.

In vitro luciferase 3′-UTR reporter assay

To confirm binding of miR-181c-5p and miR-203a-3p to the 3′-UTR of *PLS3*, a dual luciferase reporter system was applied. The 3′-UTR of human *PLS3* (transcript variant 202, ENST00000355899.8) was cloned into psiCHECK™-2 (Promega, San Luis Obispo, CA, USA). HEK293 cells, cultivated in high-glucose Dulbecco's Modified Eagle's Medium (Lonza, Basel, Switzerland) and supplemented with 2mM L-Glutamine, 10% fetal calf serum (Sigma-Aldrich, St. Louis, MO, USA), and 1% PenStrep (Sigma-Aldrich), were co-transfected with psiCHECK2-PLS3-3′-UTR and either a miRNA mimic hsa-181c-5p or hsa-203a-3p, or Negative Control #1 (mirVana™; Thermo Fisher Scientific, Waltham, MA, USA). JetPrime transfection reagent (Polyplus Transfection, New York, NY, USA) was used for transfections that were performed according to the manufacturer's protocol. Briefly, 0.25 μg/mL and 0.1 μg/mL plasmid DNA were mixed with the respective miRNA (30nM final concentration), incubated for 15 min at room temperature, and added to the cells. Medium was exchanged with fresh growth medium after 24 hours. Luciferase assay was performed 48 hours posttransfection using the Dual-Luciferase® Reporter Assay System (Promega, Madison, WI, USA) according to the manufacturer's protocol. Luminescence was measured on a Polarstar Omega (BMG Labtech, Ortenberg, Germany). *Renilla* luciferase activity was normalized against Firefly luciferase activity.

Statistical analyses

Descriptive data are given as median and range when appropriate. Statistical calculations are done by comparing both mutation-positive with mutation-negative subjects and for each gender group separately. Adjustment for other possible confounders was not reasonable due to small cohort size. We used Kolmogorov–Smirnov and Shapiro–Wilk tests to evaluate normality of data. We used unpaired two-tailed Student's *t* test and Mann–Whitney, *U* test, as appropriate (SPSS Statistics 24; IBM Corporation, Armonk, NY, USA). Values of $p < .05$ were considered statistically significant. miRNA volcano plots were drawn using effect sizes (delta–delta-Cq values) and *p* values derived from unpaired two-tailed Student's *t* test. Principal components analysis (PCA) and hierarchical clustering analysis were performed using Clustvis,[24] using delta Cq (dCq) normalized data as input values. Unit variance scaling was applied and the singular value decomposition (SVD) with imputation method, which is available with the pcaMethods package (v1.78) in R/Bioconductor (https://www.bioconductor.org/), was used. We used MedCalc Statistical Software (version 18; MedCalc Software Ltd, Ostend, Belgium; http://www.medcalc.org) to perform receiver operator characteristic (ROC) curve analysis for individual miRNAs to compute the area under the ROC curve (AUC) values. Pearson and Spearman correlation analyses and two-tailed tests were performed in GraphPad Prism v8.3.0 (GraphPad Software, Inc., La Jolla, CA, USA). Power calculations for cohort size were not considered as all available *PLS3* mutation-positive subjects and their respective mutation-negative family members were included in the study. One-way ANOVA analysis with Tukey's post hoc test was used for analysis of in vitro data. Values of *p* obtained from miRWalk 3.0 target predictions were adjusted for multiple testing using the Benjamini–Hochberg method for false-discovery rate calculation.

Results

Cohort characteristics

Mutation-positive subjects

The current study cohort comprised in total 15 *PLS3* mutation-positive subjects (five males; age range, 8–76 years; median age 41 years) (Fig. 1, Table 1). The subjects had a variable history of previous peripheral (range, 0 to >10) and vertebral compression fractures. Two subjects had sustained a peripheral fracture within the last 12 months prior to the study; to our knowledge none resulted from high-energy trauma. None of the subjects had undergone any orthopedic surgery within the last 12 months. Seven of the subjects had received prior osteoporosis medication and for two subjects, the treatment was ongoing at the time of the study; subject MP33 had received an infusion of zoledronic acid at dose 0.05 mg/kg 11 months prior to obtaining the samples, and subject MP23 had similarly received 5 mg intravenous zoledronic acid 1 month prior to the sample collection (Table 1).

Mutation-negative subjects

The control group included 17 mutation-negative subjects (eight males; age range, 8–69 years; median 41 years) (Fig. 1, Table 1). They also had a variable history of peripheral fractures (more than two fractures only in one subject) and one subject had sustained vertebral compression fractures; none of them reported recent fractures or high-energy traumas. One subject (MN36) had received prior osteoporosis medication and another subject (MN21) was receiving denosumab-injections twice a year at the time of the study. None of the subjects had had any orthopedic surgery within the last 12 months.

Clinical and biochemical characteristics

Evaluation of basic parameters of calcium-phosphate homeostasis and metabolic bone turnover markers showed generally normal findings and only isolated supra- or subnormal values in both mutation-positive and -negative subjects (Supplemental Fig. 1, Supplemental Table 1); no systematic differences were noted in relation to the subjects' mutation status, age, or gender. Serum vitamin D concentrations were similar in both groups (medians 69 versus 73 nmol/L).

miRNA quantitation quality control

Overall, there was low technical variance and low variability in data (coefficient of variation [CV]% <30) (Supplemental Fig. 2). Hemolysis index calculations detected three samples (MN27, MN29, and MN35) with ratios above a threshold of >7; they were subsequently excluded from further analyses, leaving a total number of 14 mutation-negative subjects (consisting of six males with new age median of 40 years). No samples from mutation-positive subjects were excluded for low sample quality.

Exploratory data analysis

With regard to the X chromosomal inheritance of *PLS3*, we evaluated the gender-specific effect of the *PLS3* mutations on the mutation-positive subjects' overall miRNA serum levels. We selected the 10% (ie, 20 miRNAs altogether) most upregulated or downregulated miRNAs (based on standard deviation) and

Table 1 Clinical Data for the 15 *PLS3* Mutation-Positive and 17 Mutation-Negative Subjects

Code	Family	Age category (years)	Gender	BMD			Peripheral fractures	Vertebral compression fractures	Osteoporosis medication, years since last dose	Type of osteoporosis medication	Possibly confounding medication[a]	Calcium/vitamin D supplementation
				LS	FEM	WB						
Mutation-positive subjects												
MP32	2	0–11	M	N/A	N/A	N/A	2[b]	Yes	No		No	No
MP26	1	0–11	F	N/A	N/A	N/A	0	N/A	No		No	No
MP33	3	0–11	F	−1.8	−1.9	−1.6	5	Yes	Yes[c]	ZOL	No	Yes
MP27	1	12–20	F	N/A	N/A	N/A	0	N/A	No		No	No
MP29	1	12–20	F	−2.2	−1.2	−1.1	0	No	No		Yes	No
MP31	2	21–40	M	−0.3	−1.4	−0.2	1	Yes	Yes, 9	ZOL	No	No
MP34	4	21–40	M	−3.8	−2.8	−4.5	4	Yes	No		No	Yes
MP23	1	41–60	F	−2.2	−1.5	−2.0	0	Yes	Yes[c]	ZOL	No	Yes
MP30	2	41–60	F	N/A	N/A	N/A	0	Yes	No		Yes	Yes
MP25	1	41–60	M	−1.9	−1.8	−2.5	10[b]	Yes	Yes, 7	ZOL	No	Yes
MP28	1	41–60	F	−0.6	0.5	−0.6	0	No	No		No	Yes
MP22	1	41–60	F	−1.3	N/A	−0.7	0	Yes	Yes, 5	PTH	Yes	Yes
MP35	4	41–60	F	1.2	1.1	−0.7	1	No	No		Yes	Yes
MP21	1	61–80	F	−2.3	−0.6	−1.9	>10	Yes	Yes, 4	PTH, ZOL	Yes	Yes
MP24	1	61–80	M	−2.2	N/A	−2.3	4	Yes	Yes, 6	ZOL	No	Yes
Mutation-negative subjects												
MN25	1	0–11	M	N/A	N/A	N/A	1	N/A	No		No	No
MN24	1	0–11	M	N/A	N/A	N/A	0	N/A	No		No	No
MN28	2	12–20	F	N/A	N/A	N/A	1	N/A	No		Yes	No
MN26	1	21–40	F	N/A	N/A	N/A	2	N/A	No		No	No
MN31	2	21–40	F	N/A	N/A	N/A	0	N/A	No		No	No
MN30	2	21–40	M	N/A	N/A	N/A	0	N/A	No		Yes	No
MN34	3	21–40	F	N/A	N/A	N/A	8	N/A	No		No	Yes
MN21	1	41–60	M	−1.9	−1.5	−1.9	3	Yes	Yes[c]	DMAB	No	No
MN22	1	41–60	F	0.5	−0.4	0.5	0	No	No		Yes	No
MN23	1	41–60	F	−0.1	−0.2	0.7	1	No	No		No	No
MN33	2	61–80	F	N/A	N/A	N/A	0	N/A	No		No	Yes
MN37	4	61–80	F	N/A	N/A	N/A	2	N/A	No		No	Yes
MN32	2	61–80	M	N/A	N/A	N/A	0	N/A	No		Yes	Yes
MN36	4	61–80	M	−1.3	−0.6	−1.3	0	Yes	Yes, 10	N/A	No	Yes

Mutation-positive subjects from families 1–4 harbor different *PLS3* mutations: Family a = intronic splice site mutation c.73–24T>A (p.Asp25Alafs*17); Family B = intragenic tandem duplication within *PLS3*; Family C = *de novo* heterozygous missense mutation c.1424A>G (p.Asn446Ser) in exon 12; Family D = nonsense mutation c.766C>T (p.Arg256*).

DMAB = denosumab; F = female; FEM = femoral neck; LS = lumbar spine; M = male; MN = mutation-negative; MP = mutation-positive; N/A = not available; WB = whole body; ZOL = zoledronic acid.

[a]Confounding medications include aspirin, thyroxin, glucocorticoids, risperdal/seronil, omega3.

[b]Last fracture within 12 months prior to the study.

[c]Ongoing osteoporosis medication at the time of study.

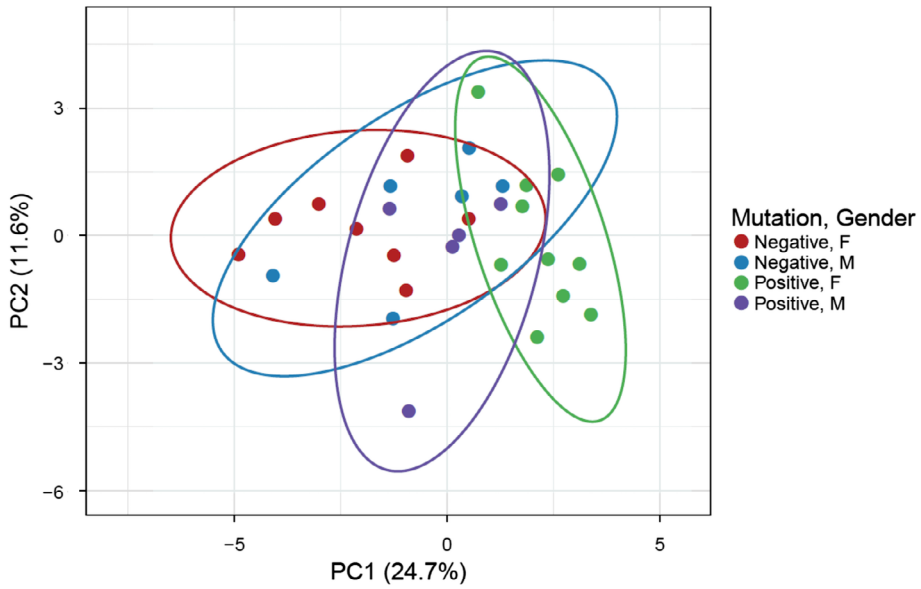

Fig 2 Principal component analysis for the top 20 most regulated miRNAs according to *p* value in 15 *PLS3* mutation-positive and 14 mutation-negative subjects. The figure shows gender-divide and grouping in the mutation-positive subjects (green versus purple), indicating gender difference in miRNA expression in *PLS3* mutation-positive subjects and altered circulating miRNA levels particularly in female mutation-positive subjects. F = female, M = male, PC = principal component.

Table 2 Differential Expression of the Top 20 Putative miRNAs in 15 *PLS3* Mutation-Positive Subjects and 14 Mutation-Negative Subjects

miRNA-ID	Regulation in MP subjects	Average normalized delta Cq		Standard deviation (Cq value)		Fold change (log_2-transformed)	Fold change (linear) MP versus MN	*p* (*t* test)			ROC analysis, AUC value
		MP	MN	MP	MN			All	Females	Males	
miR-93-3p	Down	−1.49	−0.94	0.54	0.40	−0.55	0.68	.004	.007	.344	0.812
miR-532-3p	Down	−1.60	−1.14	0.47	0.29	−0.46	0.73	.007	.027	.206	0.819
miR-133a-3p	Down	−4.91	−3.47	1.50	0.85	−1.44	0.37	.009	.042	.127	0.795
miR-301b-3p	Up	−3.42	−4.19	0.86	0.91	0.77	1.71	.015	.017	.465	0.762
miR-181c-5p	Up	−4.75	−6.20	1.82	2.28	1.45	2.73	.032	.086	.246	0.690
miR-203a-3p	Up	−5.10	−7.12	2.58	2.49	2.02	4.06	.035	.064	.454	0.726
miR-590-3p	Down	−2.75	−2.34	0.54	0.30	−0.41	0.75	.039	.021	.843	0.707
miR-23b-3p	Up	4.36	4.21	0.21	0.19	0.15	1.11	.064	.016	.682	–
miR-30c-5p	Up	2.67	2.44	0.35	0.34	0.23	1.17	.078	.086	.663	–
miR-218-5p	Up	−5.70	−7.62	2.58	2.99	1.92	3.78	.083	.132	.463	–
miR-128-3p	Up	−0.91	−1.12	0.30	0.32	0.21	1.16	.084	.011	.428	–
miR-29b-3p	Down	0.90	1.17	0.37	0.45	−0.27	0.83	.097	.020	.795	–
miR-31-5p	Down	−5.82	−4.76	1.79	1.41	−1.06	0.48	.099	.032	.712	–
miR-15b-5p	Up	2.32	2.18	0.20	0.21	0.14	1.10	.100	–	–	–
miR-423–3p	Up	1.92	1.73	0.29	0.28	0.19	1.14	.101	–	–	–
miR-96-5p	Down	−3.67	−2.23	2.95	0.88	−1.44	0.37	.103	–	–	–
miR-200b-3p	Up	−3.27	−3.85	0.87	0.99	0.58	1.49	.113	–	–	–
miR-582-3p	Down	−7.18	−5.71	2.46	2.19	−1.47	0.36	.114	–	–	–
miR-24-3p	Up	5.37	5.22	0.20	0.27	0.15	1.11	.114	–	–	–
miR-141-3p	Up	−2.23	−2.71	0.74	0.83	0.48	1.39	.123	–	–	–

miRNAs with overall *p* value < 0.05 are shown in bold. Parametric *t* test used as appropriate. For clarity, yellow indicates *p* value < 0.05 and blue indicates *p* value < 0.1.

AUC = area under the ROC curve; Cq = cycle quantification value; miRNA/miR = microRNA; MN = mutation-negative; MP = mutation-positive; ROC = receiver operator characteristic.

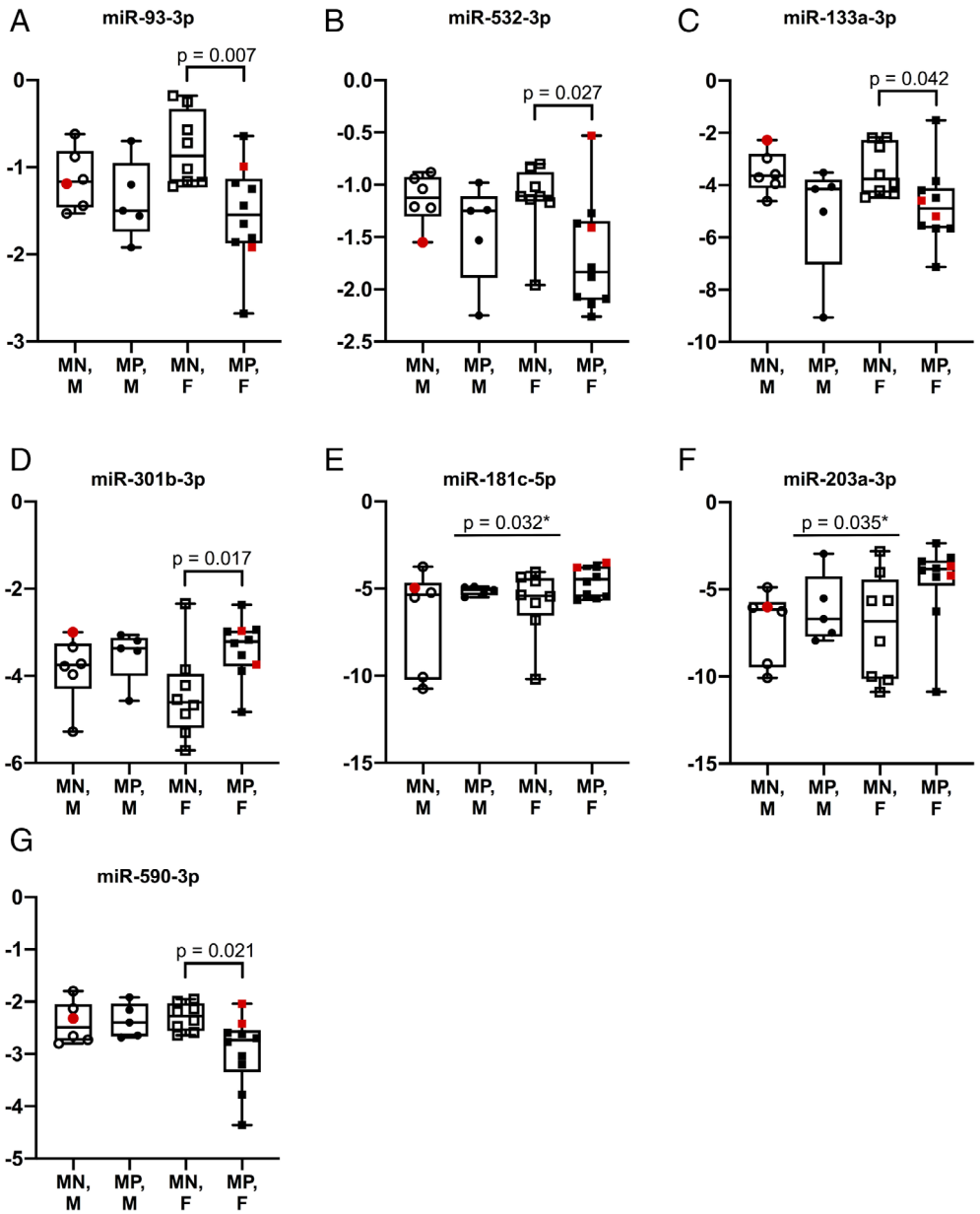

Fig 3 (*A–G*) Box plots of normalized (global mean) delta Cq values for the top seven regulated miRNAs in 15 *PLS3* mutation-positive and 14 mutation-negative subjects. Individuals with ongoing osteoporosis medication at the time of the study are indicated with red dots. Asterisk (*E,F*) refers to comparison between all MN and all MP subjects. Parametric *t* test was applied. F = female; M = male; MN = mutation-negative; MP = mutation-positive.

applied unsupervised exploratory data analyses by PCA. Principal components 1 and 2 together explained 36.3% of the overall variance but were not sufficient for complete separation of mutation-positive from mutation-negative subjects in the plot (Fig. 2). Interestingly, mutation-negative male and female subjects clustered together (Fig. 2, red versus blue), while in the mutation-positive subjects grouping by gender was observed (Fig. 2, green versus purple).

We next performed statistical analysis of the top 20 miRNA concentrations using groupwise comparisons. Of these, altogether 13 miRNAs showed a *p* value <.1 and of them, seven putative miRNAs were identified with a *p* value <.05 and were hence deemed discriminative for the mutation-positive and mutation-negative subjects (Table 2). Heat map analysis for clustering of these top 20 miRNAs showed no correlation with mutation type or subfamily division (Supplemental Figs. 3 and 4). Calculations for correlations between the top 20 miRNAs and subject age revealed that two of the miRNAs had statistically significant correlations: miR-29b-3p, *p* value .0393, and miR-141-3p, *p* value .0044 (Supplemental Table 2); neither is included in the top seven differentially expressed miRNAs.

We decided to concentrate on the top 13 miRNAs with lowest *p* values <.1 (range, .004–.099) and evaluate them in more detail (Table 2). Of these, three were statistically significantly upregulated (miR-301b-3p, miR-181c-5p, and miR-203a-3p; *p* value range, .015–.035), four were upregulated (miR-23b-3p, miR-30c-

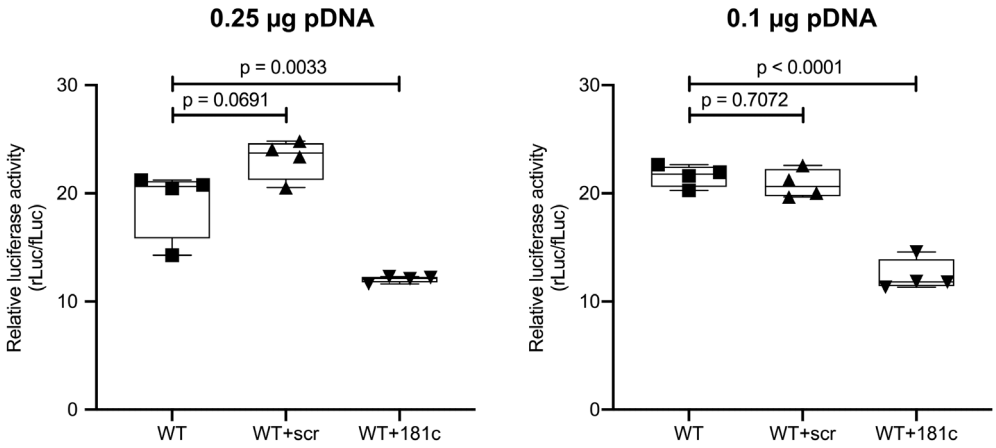

Fig 4 Luciferase reporter assay confirming posttranscriptional regulation of *PLS3* by miR-181c-5p. The experiment used a dual-luciferase reporter plasmid containing *PLS3* 3′-UTR sequence (including the putative miR-181c-5p binding site). Plasmids were transfected into HEK293 cells at two different concentrations (0.25 µg and 0.1 µg), either alone (WT), in combination with a negative control miRNA (WT+scr), or in combination with miR-181c-5p (WT+181c). One-way ANOVA analysis with Tukey's post hoc comparison was used.

Table 3 Previously Reported Data on the Role in Bone Metabolism of the Seven Discriminative miRNAs in *PLS3* Mutation-Positive Subjects

miRNA-ID	Regulation in MP subjects	Role in bone metabolism	Target proteins in bone	References
miR-93-3p	Down	Negative regulator of osteogenic differentiation; upregulated in low BMD in postmenopausal osteoporosis	RUNX2	51,52
miR-532-3p	Down	Upregulated in patients with vertebral fractures or low BMD, correlated with serum ALP	–	53
miR-133a-3p	Down	Downregulated or upregulated in mandible and femur of ovariectomized mice, respectively; upregulated in low BMD in postmenopausal osteoporosis; inhibits bone metastasis in prostate cancer	TGF-β, WNT pathway, RUNX2, CXCL11, CXCR3, SLC29A1, PI3K/AKT pathway	52–56
miR-301b-3p	Up	Upregulated in bone of placebo-treated ovariectomized rats, and downregulated following PTH treatment	–	30
miR-181c-5p	Up	Partakes in microgravity-induced abnormal osteoblast proliferation; regulated in postmenopausal osteoporotic patients	Cyclin B1	15,36
miR-203a-3p	Up	Regulates osteoblast differentiation; inhibits osteogenesis diabetic rats' jaw bones; upregulated in femoral heads and serum of ovariectomized rats, downregulation in response to anabolic treatment	DLX5, RUNX2, SMAD1	37,38,40,50
miR-590-3p	Down	Decreased expression in osteosarcoma	SOX9	57

miRNAs with overall p value < 0.05 are shown in bold.
miRNA/miR = microRNA; MP = mutation-positive.

5p, miR-218-5p, and miR-128-3p; p value range, .064–.084), four were statistically significantly downregulated (miR-532-3p, miR-590-3p, miR-93–3p, and miR-133a-3p; p value range, .004–.039), and two were downregulated (miR-29b-3p and miR-31-5p; p values .097 and .099, respectively) (Fig. 3*A*–*G*).

Ongoing osteoporosis medication at the time of the study had no systematic effect on miRNA values (Fig. 3*A*–*G*). To evaluate gender differences in miRNA levels, we evaluated the same 13 miRNAs in female and male subjects separately. When comparing miRNA concentrations between mutation-positive and mutation-negative females alone, the statistical significance persisted for expression of nine of the 13 miRNAs (miR-93-3p, miR-532-3p, miR-133a-3p, miR-301b-3p, miR-590-3p, miR-23b-3p, miR-128-3p, miR-20b-3p, and miR-31-5p; p value range, .007–.042). None of the 13 miRNAs reached a statistical significance level in males (p value range, .183–.840).

In silico prediction and in vitro confirmation of miRNA targets

First, we set out to identify putative miRNA binding sites in the human *PLS3* 3′-UTR region for these 13 specific miRNAs, with

Table 4 mRNA Targets for the Top Seven Significantly Upregulated or Downregulated Serum miRNAs (p value <.05) in 15 *PLS3* Mutation-Positive Subjects

KEGG pathway ID	KEGG pathway	Genes (n)	p	p (BH-adjusted)
hsa04350	TGF-beta signaling pathway	6	.0014	.028
hsa04360	Axon guidance	8	.0037	.037
hsa04150	mTOR signaling pathway	6	.0198	.092
hsa05205	Proteoglycans in cancer	7	.0232	.092
hsa04310	Wnt signaling pathway	6	.0172	.092
hsa04270	Vascular smooth muscle contraction	5	.0276	.092

mRNA targets were derived from miRWalk 3.0.
BH = Benjamini-Hochberg; hsa = human microRNA; KEGG = Kyoto Encyclopedia of Genes and Genomes.

binding sites conserved across mammalian species using TargetScan v7.2.[25] From the list of top 20 regulated candidates, we identified binding sites in the human *PLS3* gene for three miRNAs: miR-203a-3p, miR-181c-5p, and miR-218-5p. Of these, miR-218-5p had been experimentally validated by high-throughput sequencing of RNA isolated by crosslinking immunoprecipitation (HITS-CLIP),[26] and for miR-181c-5p and miR-203a-3p, bioinformatic predictions suggest interaction with *PLS3*. Therefore, a luciferase reporter construct containing the *PLS3* 3′-UTR was generated and tested for interaction with both miRNAs. Results for miR-181c-5p showed a clear interaction with *PLS3* 3′-UTR based on a decrease in luciferase signal compared to the negative control (Fig. 4), while the results for miR-203a-3p were inconclusive (data not shown).

To complement this analysis, mRNA targets of all seven statistically significantly upregulated or downregulated miRNAs in serum of mutation-positive subjects were derived from miRWalk 3.0. In total, 244 genes showed a putative interaction with one or more of these miRNAs. Of these genes, a strong enrichment in the TGF-beta signaling pathway (Kyoto Encyclopedia of Genes and Genomes [KEGG] hsa04350, six genes, adjusted p value .025) and WNT signaling pathway (KEGG hsa04310, six genes, adjusted p value .092) was observed (Table 4).

Discussion

This study reports for the first time on circulating levels of miRNAs in relation to defective PLS3 function. Our cohort comprised 15 subjects with different *PLS3* loss-of-function mutations leading to low BMD and frequent fragility fractures. The affected males presented with a more severe skeletal phenotype compared with the females owing to the X chromosomal inheritance of *PLS3*. We screened a custom-designed panel consisting of 192 miRNAs and compared the results with congruent findings in 14 mutation-negative subjects from the same families. Our results reveal a unique profile of seven different miRNAs that statistically significantly differ between the mutation-positive and mutation-negative subjects. Surprisingly, the difference to controls was even greater in the *PLS3* mutation-positive females than in the mutation-positive males. All seven most significantly regulated miRNAs in the mutation-positive subjects have been previously related to bone metabolism, but their association with PLS3 has not been reported.

Recently, miRNAs have attained much attention as potential markers for chronic diseases and targets for novel therapeutics. Previous reports have shown that miRNA expression levels correlate with BMD and fracture risk, relate to disease status in postmenopausal osteoporotic patients,[13,15] and can differentiate between patient cohorts in several other chronic diseases.[14,27] We have also shown that miRNA profiles can differentiate mutation-positive subjects in another monogenic skeletal disease; we found altered expression levels and a unique profile of eight differentially expressed miRNAs in a cohort of 17 *WNT1* mutation-positive subjects with autosomal dominant WNT1 osteoporosis.[8] However, serum miRNA concentrations in other monogenic disorders have hardly been explored.

Although the number of diagnosed *PLS3* mutation-positive patients has increased and the skeletal characteristics are well documented, the exact molecular mechanisms and signaling cascades in which PLS3 partakes in bone metabolism continue to be clarified. Of the seven discriminating miRNAs in our study, six have been previously reported to influence bone metabolism in humans (Table 3) and their reported roles parallel their upregulation or downregulation in the presence of mutated PLS3. For miR-301b-3p this is the first report indicating it serves a role in skeletal homeostasis in humans. Previously it has mainly been linked to hypoxic events such as hypoxia-induced carcinogenesis in prostate and other cancers[28] and pulmonary vascular proliferation and vasoconstriction in pulmonary hypertension.[29] However, recently it was reported to be linked to bone metabolism in ovariectomized rats,[30] and TargetScan also predicts it to interact directly with several bone-related proteins, such as WNT1, LRP6, and PTEN. Furthermore, miR-301b belongs to the miR-130 gene family together with miR-130b, miR-301a, and miR-130a,[31] which in turn have been reported to partake in osteogenesis and chondrogenesis.[32,33] Last, Liu and colleagues[34] have reported that expression of miR-301b-3p in bone marrow correlates with adipogenic potential of mesenchymal stem cells (MSCs).

Three miRNAs—miR-181c-5p, miR-203a-3p, and miR-218-5p—are predicted or experimentally validated to interact with or bind to PLS3. First, miR-181c-5p, which relates to postmenopausal osteoporosis and fracture risk in diabetic patients,[13,15,35] inhibits osteoblast proliferation in simulated microgravity-settings through interactions with cyclin B1.[36] Here, we could experimentally validate the interaction between miR-181c-5p and PLS3. Second, miR-203a-3p is reported to regulate osteoblast differentiation through repressing DLX5 and RUNX2 in traumatic heterotopic ossification and in bone lesions of metastatic breast cancer,[37–39] and to inhibit osteogenesis in diabetic rats' jaw bones.[40] The role of miR-203a-3p in bone metabolism and its inhibitory functions on bone formation are quite well established and in the light of our results, it could be hypothesized that some of its regulatory actions are transmitted through interactions with PLS3. Last, miR-218-5p has been stated to promote osteogenic differentiation of MSCs in mice[41] and increase bone formation by targeting WNT pathway inhibitors,[42] all the while also negatively regulating osteoclastogenesis through RANKL, Mmp9, and NF-κB.[43,44]

Of note, we have recently published findings of elevated serum Dickkopf-1 (DKK1; dickkopf WNT signaling pathway inhibitor 1) concentrations in these same *PLS3* mutation-positive subjects.[45] DKK1 is an osteocyte-derived inhibitor of the WNT pathway in bone. It downregulates WNT signaling by binding to LRP5,[46] preventing binding of a WNT ligand. Although the mechanisms behind the molecular interactions between PLS3 and DKK1 are still unknown, interestingly two of our upregulated miRNAs of interest also target DKK1. miR-203 promotes osteogenic differentiation of MSCs by inhibiting and degrading DKK1[47] and, similarly, miR-218-5p promotes osteogenic differentiation of synovium-derived fibroblast-like cells in rheumatoid arthritis by suppressing DKK1.[48] Further, we noticed enrichment in the WNT pathway when looking at mRNA targets for the seven top miRNAs (Table 4). Interestingly, four of the significantly expressed miRNAs in this study (miR-31-5p, miR-200b-3p, miR-423–3p, miR-128-3p) also showed differential expression in our previous study on miRNAs in WNT1 osteoporosis,[8] with p values <.1 for each miRNA in both cohorts. The molecular associations between these miRNAs and PLS3 still need further consideration.

We noticed a difference between genders, with the mutation-positive females having more significant changes than the mutation-positive males in comparison to corresponding mutation-negative subjects. Due to the X-linked inheritance pattern, PLS3 osteoporosis predominantly affects males whereas female carriers exhibit a much milder phenotype.[18,19] Therefore, this counterintuitive finding is interesting yet unclear. Some of the differences between mutation-positive and mutation-negative males could be downplayed by their relatively small cohort size compared to females (5 versus 10). However, prior studies congruently report gender differences in PLS3 function. For example, PLS3 has been reported to be a gender-specific modifier in spinal muscular atrophy.[49,50] We also found a similar gender-dependent difference in circulating DKK1 concentrations, *PLS3* mutation-positive females showing significantly elevated and greater concentrations than males when compared with mutation-negative female controls.[45]

Prior or ongoing osteoporosis medication could potentially introduce bias on miRNA expression levels.[30] Our cohort included altogether six subjects with previous, and three subjects with ongoing osteoporosis treatment at the time of the study. However, separate analysis indicated no relationship between treatment and miRNA levels. This is similar to our previous observation in miRNAs in WNT1 osteoporosis.[8]

We also acknowledge other limitations our study may have, mainly concerning the relatively small cohort size, heterogeneity of *PLS3* mutations, and the cross-sectional nature of the study. A greater number of study subjects with similar mutations, and exclusion of mutation-negative subjects with a positive fracture history or osteoporosis would perhaps better reflect the true difference in miRNA expression levels in PLS3 osteoporosis and solidify the observed gender differences. A longitudinal study setting would allow to evaluate the changes in miRNA levels with respect to disease progression or treatment response and assess their potential as biomarkers. Also, although relatively inclusive, our panel consisted of only 192 miRNA species, which could count out some important and bone-specific or relevantly expressed miRNAs. Because of the exploratory nature of this study we purposely decided to apply relaxed statistical cutoffs (ie, no adjustment for multiple testing), which could have resulted in a higher false-positive rate, and, thus, the results will require independent confirmation. Further, we recognize some potential confounding factors that could introduce bias, such as other medications or illnesses. The medication intakes, however, were similar in both groups and the two groups were otherwise highly alike with regard to age, gender, and family and genetic background. Furthermore, given the rarity of PLS3 osteoporosis, the scarce number of *PLS3* mutation-positive subjects, and the unknown pathomechanisms behind PLS3-related bone disease, we consider our study topic relevant and current, and the findings scientifically novel and greatly valuable.

In conclusion, our study identified a specific pattern of circulating miRNAs in *PLS3* mutation-positive subjects. These findings imply that there is possible crosstalk between PLS3 and specific miRNAs in bone metabolism and that the identified miRNAs could contribute to the skeletal pathology in PLS3 osteoporosis. Importantly, several of these miRNAs show association with the WNT pathway, an observation which may have relevance in understanding the pathomechanisms underlying PLS3 osteoporosis and in advancing patient management. Because conventional metabolic bone markers are normal in *PLS3* mutation-positive subjects, our findings could provide novel avenues for utilizing miRNAs as biomarkers in diagnosing and monitoring patients. These miRNAs may also be explored as therapeutic targets to improve skeletal health by influencing PLS3 signaling.

Disclosures

MH and JG are co-founders of TAmiRNA. MH and MW are employed by TAmiRNA. JG is a scientific advisor to TAmiRNA. MH and JG hold patents related to the application of circulating microRNAs as biomarkers for diagnosis of bone disorders. OM declares consultancy to Kyowa Kirin, Alexion, and Sandoz. The REM, MW, AF, AK, AC and OM have declared that no conflicts of interest exist.

Acknowledgments

This study was supported by the Sigrid Jusélius Foundation, the Novo Nordisk Foundation, the Folkhälsan Research Foundation, the Academy of Finland, the Foundation for Pediatric Research, the Helsinki University Research Funds, Helsinki University, and Helsinki University Hospital through the Doctoral Programme in Clinical Research, the Orion Research Foundation, the Finnish Otorhinolaryngology–Head and Neck Surgery (ORL–HNS) Foundation, the Päivikki and Sakari Sohlberg Foundation, the Finnish–Norwegian Medical Foundation, the Jalmari and Rauha Ahokas Foundation, the Juhani Aho Foundation, the Swedish Research Council, the Swedish Childhood Cancer Foundation, Konung Gustaf V:s och Drottning Victorias Frimurarestiftelse, Stockholm County Council, and Karolinska Institutet. The funders had no role in the design and conduct of the study; collection, management, analysis, and interpretation of the data; and preparation, review, or approval of the manuscript. We thank Päivi Turunen and Kirsi Mäkelä-Kvist for their help with collecting subject and sample data, and Susanna Skalicky for excellent technical support.

Authors' roles: Study design: REM, MH, JG, and OM. Study conduct: REM, MH, JG, and OM. Data collection: REM, MW, AC, AK, MH, and JG. Data analysis: REM, MW, MH, and JG. Drafting manuscript: REM and MH. Revising manuscript content: all authors. Approving final version of manuscript: all authors. REM, MH, JG, and OM take responsibility for the integrity of the data.

Peer Review

The peer review history for this article is available at https://publons.com/publon/10.1002/jbmr.4097.

References

1. Trajanoska K, Rivadeneira F. The genetic architecture of osteoporosis and fracture risk. Bone. 2019;126:2–10.
2. Styrkarsdottir U, Stefansson OA, Gunnarsdottir K, et al. GWAS of bone size yields twelve loci that also affect height, BMD, osteoarthritis or fractures. Nat Commun. 2019;10:2054.
3. Morris JA, Kemp JP, Youlten SE, et al. An atlas of genetic influences on osteoporosis in humans and mice. Nat Genet. 2019;51:258–66.
4. Rivadeneira F, Mäkitie O. Osteoporosis and bone mass disorders: from gene pathways to treatments. Trends Endocrinol Metab. 2016; 27:262–81.
5. Ralston SH, Uitterlinden AG. Genetics of osteoporosis. Endocr Rev. 2010;31:629–62.
6. van Wijnen AJ, van de Peppel J, van Leeuwen JP, et al. MicroRNA functions in osteogenesis and dysfunctions in osteoporosis. Curr Osteoporos Rep. 2013;11:72–82.
7. Zhao X, Xu D, Li Y, et al. MicroRNAs regulate bone metabolism. J Bone Miner Metab. 2014;32:221–31.
8. Mäkitie RE, Hackl M, Niinimäki R, Kakko S, Grillari J, Mäkitie O. Altered MicroRNA profile in osteoporosis caused by impaired WNT signaling. J Clin Endocrinol Metab. 2018;103:1985–96.
9. Bartel DP. MicroRNAs: genomics, biogenesis, mechanism, and function. Cell. 2004;116:281–97.
10. Lauressergues D, Couzigou J, Clemente HS, et al. Primary transcripts of microRNAs encode regulatory peptides. Nature. 2015;520:90–3.
11. John B, Enright AJ, Aravin A, Tuschl T, Sander C, Marks DS. Human microRNA targets. PLoS Biol. 2004;2:e363.
12. Lian JB, Stein GS, van Wijnen AJ, et al. MicroRNA control of bone formation and homeostasis. Nat Rev Endocrinol. 2012;8:212–27.
13. Heilmeier U, Hackl M, Skalicky S, et al. Serum miRNA signatures are indicative of skeletal fractures in postmenopausal women with and without type 2 diabetes and influence osteogenic and adipogenic differentiation of adipose tissue-derived mesenchymal stem cells in vitro. J Bone Miner Res. 2016;31:2173–92.
14. Hackl M, Heilmeier U, Weilner S, Grillari J. Circulating microRNAs as novel biomarkers for bone diseases—complex signatures for multifactorial diseases? Mol Cell Endocrinol. 2016;432:483–95.
15. Kocijan R, Muschitz C, Geiger E, et al. Circulating microRNA signatures in patients with idiopathic and postmenopausal osteoporosis and fragility fractures. J Clin Endocrinol Metab. 2016;101:4125–34.
16. van Dijk FS, Zillikens MC, Micha D, et al. PLS3 mutations in X-linked osteoporosis with fractures. N Engl J Med. 2013;369:1529–36.
17. Kämpe AJ, Costantini A, Levy-Shraga Y, et al. PLS3 deletions lead to severe spinal osteoporosis and disturbed bone matrix mineralization. J Bone Miner Res. 2017;32:2394–404.
18. Kämpe AJ, Costantini A, Mäkitie RE, et al. PLS3 sequencing in childhood-onset primary osteoporosis identifies two novel disease-causing variants. Osteoporos Int. 2017;28:3023–32.
19. Laine CM, Wessman M, Toiviainen-Salo S, et al. A novel splice mutation in PLS3 causes X-linked early onset low-turnover osteoporosis. J Bone Miner Res. 2015;30:510–8.
20. Costantini A, Skarp S, Kämpe A, et al. Rare copy number variants in array-based comparative genomic hybridization in early-onset skeletal fragility. Front Endocrinol. 2018;9:380.
21. Mäkitie RE, Costantini A, Kämpe A, Alm JJ, Mäkitie O. New insights into monogenic causes of osteoporosis. Front Endocrinol. 2019; 10:70.
22. Blondal T, Jensby Nielsen S, Baker A, et al. Assessing sample and miRNA profile quality in serum and plasma or other biofluids. Methods. 2013;59:S1–6.
23. Sticht C, De La Torre C, Parveen A, Gretz N. miRWalk: an online resource for prediction of microRNA binding sites. PLoS One. 2018; 13(10):e0206239.
24. Metsalu T, Vilo J. ClustVis: a web tool for visualizing clustering of multivariate data using principal component analysis and heatmap. Nucleic Acids Res. 2015;43:W566–70.
25. Agarwal V, Bell GW, Nam JW, Bartel DP. Predicting effective microRNA target sites in mammalian mRNAs. Elife. 2015;4:e05005.
26. Venkataraman S, Birks DK, Balakrishnan I, et al. MicroRNA 218 acts as a tumor suppressor by targeting multiple cancer phenotype-associated genes in medulloblastoma. J Biol Chem. 2013;288: 1918–28.
27. Beyer C, Zampetaki A, Lin NY, et al. Signature of circulating microRNAs in osteoarthritis. Ann Rheum Dis. 2015;74:e18.
28. Zheng H, Bai L. Hypoxia induced microRNA-301b-3p overexpression promotes proliferation, migration and invasion of prostate cancer cells by targeting LRP1B. Exp Mol Pathol. 2019;111: 104301.
29. Bertero T, Cottrill K, Krauszman A, et al. The microRNA-130/301 family controls vasoconstriction in pulmonary hypertension. J Biol Chem. 2015;290:2069–85.
30. Kocijan R, Weigl M, Skalicky S, et al. MicroRNA levels in bone and blood change during bisphosphonate and teriparatide therapy in an animal model of postmenopausal osteoporosis. Bone. 2020;131: 115140.
31. Fort RS, Mathó C, Oliveira-Rizzo C, Garat B, Sotelo-Silveira JR, Duhagon MA. An integrated view of the role of miR-130b/301b miRNA cluster in prostate cancer. Exp Hematol Oncol. 2018;7:10.
32. Suomi S, Taipaleenmäki H, Seppänen A, et al. MicroRNAs regulate osteogenesis and chondrogenesis of mouse bone marrow stromal cells. Gene Regul Syst Biol. 2008;2:177–91.
33. Seenprachawong K, Tawornsawutruk T, Nantasenamat C, Nuchnoi P, Hongeng S, Supokawej A. miR-130a and miR-27b enhance osteogenesis in human bone marrow mesenchymal stem cells via specific down-regulation of peroxisome proliferator-activated receptor γ. Front Genet. 2018;9:543.
34. Liu J, Xing Y, Rong L. miR-181 regulates cisplatin-resistant non-small cell lung cancer via downregulation of autophagy through the PTEN/PI3K/AKT pathway. Oncol Rep. 2018;39:1631–9.
35. Ma J, Lin X, Chen C, et al. Circulating miR-181c-5p and miR-497-5p are potential biomarkers for prognosis and diagnosis of osteoporosis. J Clin Endocrinol Metab. 2020;105:300.
36. Sun Z, Li Y, Wang H, et al. miR-181c-5p mediates simulated microgravity-induced impaired osteoblast proliferation by promoting cell cycle arrested in the G(2) phase. J Cell Mol Med. 2019;23: 3302–16.
37. Tu B, Liu S, Yu B, et al. miR-203 inhibits the traumatic heterotopic ossification by targeting Runx2. Cell Death Dis. 2016;7:e2436.
38. Laxman N, Mallmin H, Nilsson O, Kindmark A. miR-203 and miR-320 regulate bone morphogenetic protein-2-induced osteoblast differentiation by targeting distal-less Homeobox 5 (Dlx5). Genes. 2016; 8:4.
39. Taipaleenmäki H, Browne G, Akech J, et al. Targeting of Runx2 by miR-135 and miR-203 impairs progression of breast cancer and metastatic bone disease. Cancer Res. 2015;75:1433–44.
40. Tang Y, Zheng L, Zhou J, et al. miR-203–3p participates in the suppression of diabetes-associated osteogenesis in the jaw bone through targeting Smad1. Int J Mol Med. 2018;41: 1595–607.
41. Shi L, Feng L, Liu Y, et al. MicroRNA-218 promotes osteogenic differentiation of mesenchymal stem cells and accelerates bone fracture healing. Calcif Tissue Int. 2018;103:227–36.
42. Hassan MQ, Maeda Y, Taipaleenmaki H, et al. miR-218 directs a Wnt signaling circuit to promote differentiation of osteoblasts and osteomimicry of metastatic cancer cells. J Biol Chem. 2012;287: 42084–92.
43. Guo J, Zeng X, Miao J, et al. MiRNA-218 regulates osteoclast differentiation and inflammation response in periodontitis rats through Mmp9. Cell Microbiol. 2019;21:e12979.

44. Wang W, Yang L, Zhang D, et al. MicroRNA-218 negatively regulates osteoclastogenic differentiation by repressing the nuclear factor-κB signaling pathway and targeting tumor necrosis factor receptor 1. Cell Physiol Biochem. 2018;48:339–47.
45. Mäkitie RE, Kämpe A, Costantini A, Alm JJ, Magnusson P, Mäkitie O. Biomarkers in WNT1 and PLS3 osteoporosis: altered concentrations of DKK1 and FGF23. J Bone Miner Res. 2020;35:901–12.
46. Baron R, Kneissel M. WNT signaling in bone homeostasis and disease: from human mutations to treatments. Nat Med. 2013;19:179–92.
47. Xia ZL, Wang Y, Sun QD, Du XF. MiR-203 is involved in osteoporosis by regulating DKK1 and inhibiting osteogenic differentiation of MSCs. Eur Rev Med Pharmacol Sci. 2018;22:5098–105.
48. Iwamoto N, Fukui S, Takatani A, et al. Osteogenic differentiation of fibroblast-like synovial cells in rheumatoid arthritis is induced by microRNA-218 through a ROBO/slit pathway. Arthritis Res Ther. 2018;20:189.
49. Yanyan C, Yujin Q, Jinli B, Yuwei J, Hong W, Fang S. Correlation of PLS3 expression with disease severity in children with spinal muscular atrophy. J Hum Genet. 2014;59:24–7.
50. Oprea GE, Kröber S, McWhorter ML, et al. Plastin 3 is a protective modifier of autosomal recessive spinal muscular atrophy. Science. 2008;320:524–7.
51. Peng W, Zhu SX, Wang J, Chen LL, Weng JQ, Chen SL. Lnc-NTF3-5 promotes osteogenic differentiation of maxillary sinus membrane stem cells via sponging miR-93-3p. Clin Implant Dent Relat Res. 2018;20:110–21.
52. Feng Q, Zheng S, Zheng J. The emerging role of microRNAs in bone remodeling and its therapeutic implications for osteoporosis. Biosci Rep. 2018;38:BSR20180453.
53. Zarecki P, Hackl M, Grillari J, Debono M, Eastell R. Serum microRNAs as novel biomarkers for osteoporotic vertebral fractures. Bone. 2020;130:115105.
54. Tang Y, Pan J, Huang S, et al. Downregulation of miR-133a-3p promotes prostate cancer bone metastasis via activating PI3K/AKT signaling. J Exp Clin Cancer Res. 2018;37:160.
55. Hao L, Li J, Tian Y, Wu J. Changes in the microRNA profile of the mandible of ovariectomized mice. Cell Physiol Biochem. 2016;38:1267–87.
56. Wang Y, Li L, Moore BT, et al. MiR-133a in human circulating monocytes: a potential biomarker associated with postmenopausal osteoporosis. PLoS One. 2012;7:e34641.
57. Wang WT, Qi Q, Zhao P, Li CY, Yin XY, Yan RB. miR-590-3p is a novel microRNA which suppresses osteosarcoma progression by targeting SOX9. Biomed Pharmacother. 2018;107:1763–9.